DRIVE LEVEL DEPENDENCE IN QUARTZ CRYSTAL RESONATORS AT LOW DRIVE LEVELS: A REVIEW

R. Brendel [a], M. Addouche [b], P. Salzenstein [a], E. Rubiola [c], and Y. S. Shmaliy [d]

[a] FEMTO–ST – Laboratoire de Physique et Métrologie des Oscillateurs
32, avenue de l'Observatoire – F25044 Besançon cedex – France
brendel@lpmo.edu – Fax +33 (0)3 81 95 39 98

[b] Laboratoire d'Astrophysique de l'Observatoire de Besançon
41, avenue de l'Observatoire – F25030 Besançon cedex – France

[c] ESSTIN – LPMI Université H. Poincaré
2, avenue Jean Lamour – F54519 Vandœuvre lès Nancy – France

[d] FIMEE Guanajuato University
p.o. Box 215-A, Prol. Tampico S/N 36790, Salamanca Gto – Mexico

Keywords: Quartz, Resonator, Drive Level Sensitivity

Abstract

Usually, starting of oscillation in a quartz crystal oscillator requires a resonator's input power in the range of – 20 dBm, but under storage a phenomenon known as Drive Level Dependency (DLD) or Drive Level Sensitivity (DLS) may appear that prevents the starting of oscillation. Several studies performed in the past have shown that at low drive level some quartz resonators may exhibit a large increase of their series resistance preventing the starting of oscillation. This work reviews the studies and results obtained for nearly fifty years on very low drive level sensitivity of quartz. The various mechanisms and models based on the hypothesis of moving particles and surface defects in the resonator inducing resistance increase and its relation with noise mechanism are reviewed as well. Also, the paper describes several experimental set-ups, and measurement procedures used to obtain very low drive level motional parameters. This work is a contribution to understand the problem of starting quartz after a long storage period. Some preliminary results of the series resistance measured at very low drive level are also presented.

1 Introduction

For about fifty years, engineers and manufacturers have been faced with the particular behaviour of certain oscillators that do not start despite the fact that the resonator's parameters meet the specifications at normal drive level [3]. It was found that the reason why this happens comes from a large increase of the resonator's series resistance at low drive level that cannot be compensated by the negative resistance of the feedback amplifier [12]. The number of names this phenomenon has been given shows that it is very common: authors often refer to "Starting Resistance" [3], "Hard Starting Characteristics", "Sleeping Sickness" [4], "Current Dependency of Crystal Resistance" [21], "Low Level Drive Sensitivity" [8], "Second Level of Drive" [15]. Although the name "Drive Level Dependency" [29] is widely used in this context, it is often used to mean the anisochronism effect occurring at high drive level, to avoid misunderstanding with this non-linear phenomenon that has a quite different origin, it seems wiser to use a different expression such as "Drive Level Sensitivity" (DLS) [10] used here[1]. Very early, DLS has been attributed to surface defects coming from microscopic scraps of various origin often associated with a sticky surface coating [3] or surface scratches [8,21]. The increase of the resonator series resistance is one of the most obvious effects of these surface defects, but other parasitic effects should have the same origin such as intermodulation in monolithic filters [8,14], ageing [4,6], frequency jumps [10], or noise [2,10,30]. On the other hand, the extreme sensitivity of the resonator characteristics to a tiny surface modification has been turned to account by using it as a sensor for the characterization of bonding forces between a surface and gold particles [9], stainless steel [31], or polystyrene spheres [16].

2 DLS behaviour and characteristics

Many experiments have been reported during several decades, some of the most demonstrative will be summarized here. For example, a monotonic decrease of the series resistance as the drive level increase (Fig. 1) [21], sometime, series resistance starts low, increases up to a maximum then decreases (Fig. 2) [21], most of the time, the phenomenon is not reversible, and exhibits an hysteresis with unpredictable threshold as shown in Fig. 3 [21]. Note that the resistance change is accompanied with a change of the resonance frequency either negative or positive as in this figure. Also, asymmetrical behaviour as shown in Fig. 4 has been reported [8].

[1] A more rigorous and unambiguous definition of the effect would require to call it "Low drive levels DLD" or "DLD at low drive levels". Here the term "Drive Level Sensitivity" or DLS should be considered only as a short cut.

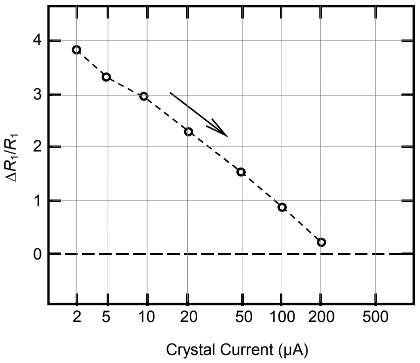

Figure 1: Monotonic decrease [21].

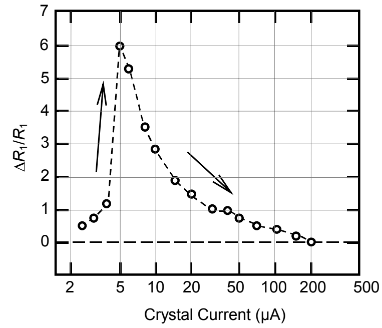

Figure 2: Maximum resistance for a particular drive level [21].

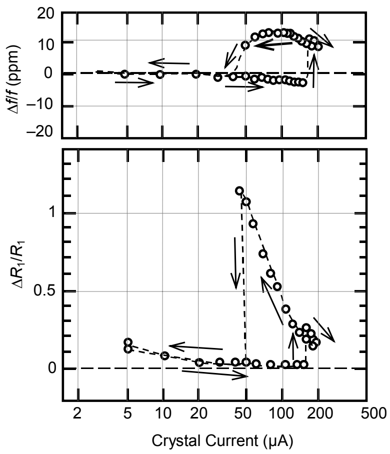

Figure 3: Hysteresis of the resonance frequency and series resistance [21].

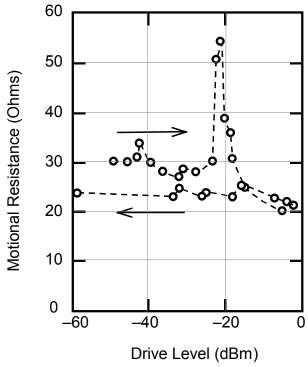

Figure 4: Peak and hysteresis of the series resistance [8].

A large number of experiments carried out for decades have led to the following observations:

- Increase of the series resistance is always associated with a positive or negative frequency shift.
- The DLS "signature" strongly depends on the temperature [21].
- The DLS behaviour can be modified or suppressed permanently or temporarily by overdriving the resonator [3,21], by polishing, etching or cleaning the crystal, this latter process being often considered as the most efficient [7,15].
- The most frustrating aspect of this phenomenon is its lack of reproducibility, hence crystals seemingly identical may be drive sensitive or not, and DLS of crystals apparently cured may reappear after a long time of inactivity.

3 Origin of the DLS

A lot of works and efforts have been put into understanding the origin of the phenomenon, and very early the attention has been focused on the surface imperfections as a possible cause of the DLS. Among the most often reported surface defects involved one can cite:

- Particles of metal or quartz or abrasive,
- Thin coat of resin or oil,
- Surface scratches,
- Flaking of quartz surface or metal electrode,
- Poorly adhesive electrodes or blisters,
- Surface stress.

Various experiments have proved the relationship of cause and effect between the surface pollution and DLS. For example, talc blown in the vicinity of an unsealed quartz resonator may induce DLS [5]. Another interesting and dramatic demonstration of the correlation between surface contamination and DLS has been reported a few years ago [6]: small squares in Figure 6 is a record of the relative resistance vs. drive level of a 100 MHz 5^{th} overtone AT-cut crystal that doesn't exhibit a noticeable DLS. The same resonator has been opened and the surface has been sprinkled with alumina particles as shown in Fig. 5, after the resonator has been resealed, it presents an important DLS (small circles in Fig. 6). Once the resonator has been reopened, cleaned and resealed, it approximately recovered its original state (small triangles in Fig. 6).

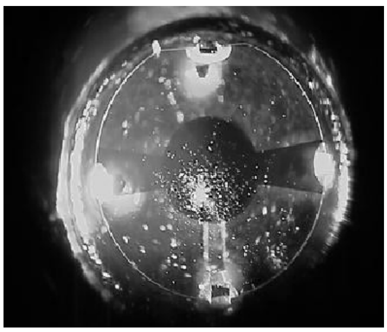

Figure 5: Particles of alumina on the surface of a resonator [6].

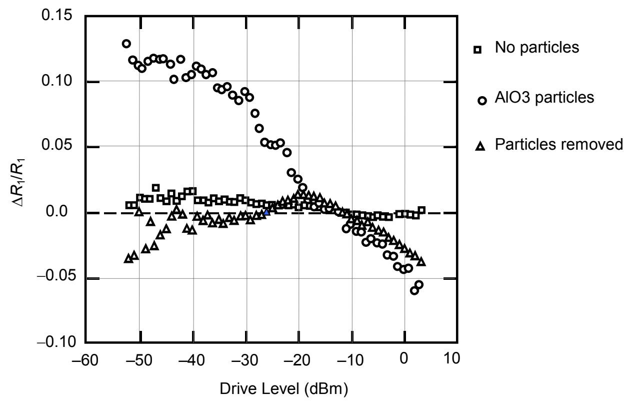

Figure 6: Effect of a surface contamination [6].

4 Mechanism of the DLS

Many attempts have been made to explain the mechanism responsible for the DLS. It should be noted first that a particle by oneself, that is without any bound with the surface, cannot induce the observed phenomena. On the other hand, if the particle were tightly bound to the surface, it would act as a mass loading and should induce a negative frequency shift which is often refuted by experiments. So, observed phenomena can be explained only if the particle is bound to the surface by an elastic force that can be due to a thin sticky coating of oil or resin, or any other attractive force such as Van der Waals, electrostatic, capillarity forces for example [31] (Fig. 7). In this case, as the surface moves back and forth under the shear motion, the bounded particle acts as a small oscillating system (Fig. 7c).

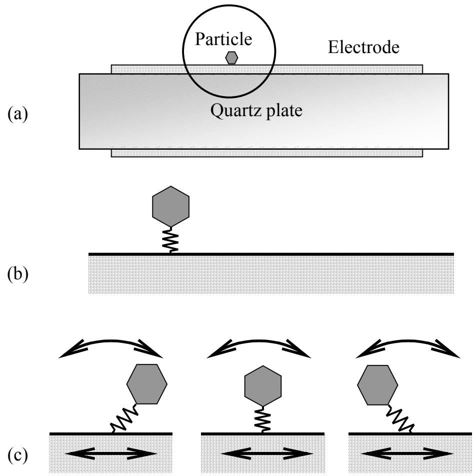

Figure 7: Particle bound to the surface by an elastic force.

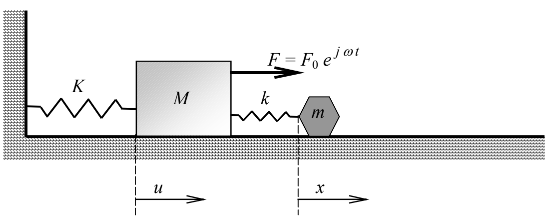

Figure 8: Simple mechanical model [9].

4.1 Simple mechanical model

A simple model of coupled oscillators has been proposed on the basis of a mechanical analogy represented in Fig. 8 [9]. The large spring–mass system at left mimics the resonator motion, while the small one at right represents the particle motion. The shear motion of the surface acts as an external driving force F. Using Newton's law with the system parameters defined here, the motion of the two masses can be obtain under the form of a differential system [Equation (1)].

$$\begin{cases} M\ddot{u} + Ku + k\,(u - x) = F_0 e^{j\omega t} \\ m\ddot{x} + k\,(x - u) = 0 \end{cases} \tag{1}$$

Searching a harmonic solution of the system, the resonant frequency of the coupled system [Equation (2)] can be expressed as a function of the resonant frequencies of the isolated spring–mass systems and of the stiffness ratio α [Equation (3)].

$$\omega_c^2 = \frac{\omega_p^2 + (1+\alpha)\omega_r^2}{2}\left[1 \pm \sqrt{1 - \frac{4\omega_p^2\omega_r^2}{\omega_p^2 + (1+\alpha)\omega_r^2}}\,\right] \tag{2}$$

$$\omega_p^2 = \frac{k}{m} \qquad \omega_r^2 = \frac{K}{M} \qquad \alpha = \frac{k}{K} \tag{3}$$

By plotting the coupled system resonant frequency as a function of the stiffness ratio, it turns out in Fig. 9 that for a weak particle binding the resonant frequency should increase while for a strong coupling, the frequency should decrease as for the mass loading effect.

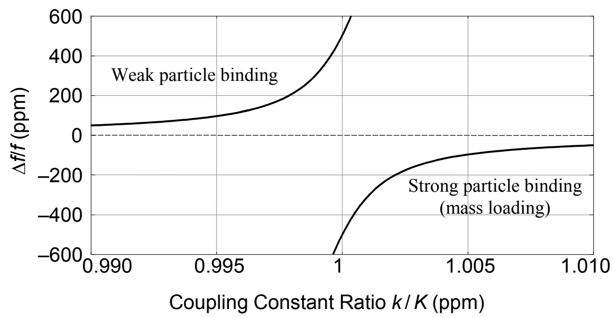

Figure 9: Resonant frequency of the coupled system.

4.2 Surface trapped particle model

Although the simple coupling system we just presented does explain that the resonant frequency can either decrease or increase, it doesn't give information on the damping mechanism. Even if linear damping terms were introduced in the resonator and particle spring–mass equivalent systems, they would induce a linear equivalent damping term independent of the drive level. Thus, a drive level sensitive damping term must invoke some non-linear mechanism such as proposed by Dworsky [8] assuming that the particles trapped in some surface imperfections should experience inelastic collisions with scratch walls as illustrated in Fig. 10 for example, thus inducing the required non-linear damping term.

Figure 11 shows the mechanical equivalent coupled oscillator that looks like the previous one with damping terms added to the spring–mass system.

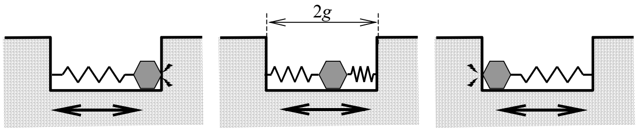

Figure 10: Surface trapped particle [8].

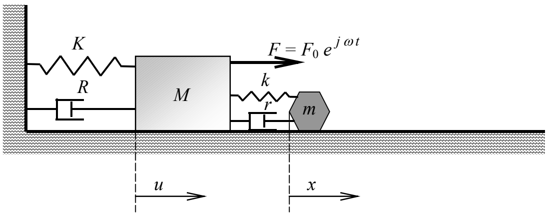

Figure 11: Mechanical equivalent of a trapped particle [8].

Motion Equations (4) are derived from the Newton's law where the particle damping factor has been given the form of Equation (5) suggested by some statistical and physical considerations.

$$\begin{cases} M\ddot{u} + R\dot{u} + Ku + k\,(u - x) + r\,(\dot{u} - \dot{x}) = F_0 e^{j\omega t} \\ m\ddot{x} + k\,(x - u) + r\,(\dot{x} - \dot{u}) = 0 \end{cases} \tag{4}$$

$$r = r_0\left[1 + \left(\frac{x - u}{g}\right)^n\right] \tag{5}$$

The mechanical coupled system previously presented has an electrical equivalent circuit represented in Fig. 12 where the non-linear damping term of the particle is modelled by a non-linear resistor the resistance of which depends on the driving current [Equation (6)].

$$r = r_0\left[1 + \left(\frac{i(r)}{g}\right)^n\right] \tag{6}$$

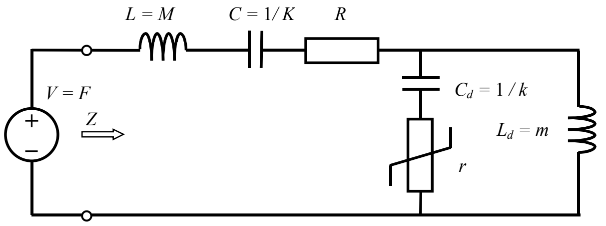

Figure 12: Electrical equivalent of a trapped particle [8].

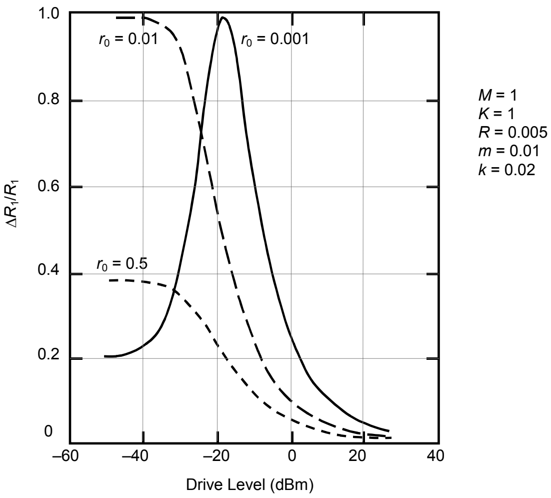

Figure 13: Modelling of a drive level sensitive resistance [8].

The equivalent resistance of the coupled system can be obtained from the real part of the equivalent impedance Z calculated by using numerical method. According to the value given to the linear particle damping term r_0, Fig. 13 shows that the model satisfactorily depicts various behaviours observed experimentally except the hysteresis phenomenon.

4.3 Physical model

Up to now, the models used give only qualitative explanations on the observed phenomenon. By using a physical distributed model for the resonator [10] it is possible to express its electrical admittance under the form given by Equation (7) where the first term of the right hand side represents the series–branch admittance. The parameter K_q depends on the geometry, on the physical constants, on the orientation, and on the particular vibration mode of the crystal plate. The second term is the static or parallel capacitance of the resonator. In this model, the crystal losses are introduced under the form of an imaginary part in the expression of the series resonant frequency [Equation (8)].

$$Y = \frac{j\omega K_q}{\omega_s^2 - \omega^2} + j\omega C_0 \tag{7}$$

$$\omega_s = \omega_s^r + j\omega_s^i \tag{8}$$

The influence of a particle located on the resonator can be calculated assuming it acts as a small spring–mass–dashpot system inducing an equivalent surface force F as shown in Fig. 14.

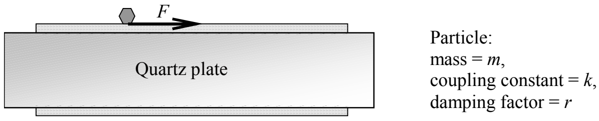

Figure 14: Action of a lumped spring–mass–dashpot particle on a distributed resonator model [10].

In this case, it can be shown that the particle introduces a perturbation term in the denominator of the series–branch admittance [Equation (9)], that has the form given by Equation (10). The perturbation term can be expressed as a function of the particle resonant frequency, and the mass ratio of the particle to the mass of the actively vibrating quartz region [Equation (11)].

$$Y = \frac{j\omega K_q}{\omega_s^2 - \omega^2 - \dfrac{2F}{mu}} + j\omega C_0 \tag{9}$$

$$\frac{2F}{mu} = 2\alpha\,\frac{\omega^2\left(\omega_p^2 + j\omega\dfrac{r}{m}\right)}{\omega_p^2 - \omega^2 + j\omega\dfrac{r}{m}} \tag{10}$$

$$\alpha = \frac{m}{M} \qquad \omega_p^2 = \frac{k}{m} \tag{11}$$

Figure 15 shows the relative series resistance change of the resonator as a function of the particle damping to mass ratio for two values of the particle to resonator mass ratio. Note that a mass ratio of only 1 ppm would induce a 100 % increase of the series resistance and this value would dramatically increase if the particle resonant frequency is close from the resonator one.

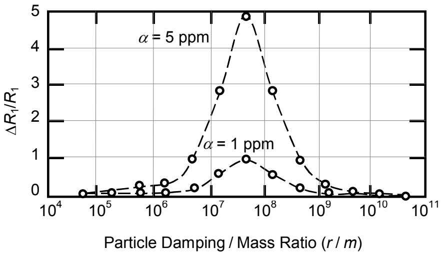

Figure 15: Physical modelling of a drive level sensitive resistance [10].

Besides of its influence on the pure shear mode equivalent admittance previously described, a localized irregularity can also be responsible for resonant mode distortions due to small parasitic flexural motions that induce additional vibration energy losses [11]. Furthermore, the strong dependence of the parasitic effect with the particular location of the irregularity should explain the hysteresis or other irreproducible behaviour of the DLS as well as the high drive level curing mechanism [10].

5 Experimental methods and results

From the experimental point of view, several methods can be used to measure DLS. In the earliest experiments, the crystal impedance meter was the most common method used [3]. Then, an easier way was to use an oscillator with variable gain as schematically depicted in Fig. 16. At low gain, the negative resistance of the amplifier cannot compensate for the resonator loss so that the oscillator doesn't start. By progressively increasing the amplifier gain up to reach the oscillation level it is possible to know if the crystal is drive level sensitive or not. Nevertheless, this fast and inexpensive method doesn't give dependency with drive level and is mainly used for screening of crystals to specified acceptance limits. [17,29].

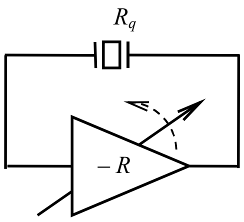

Figure 14: Active method for DLS measurement [29].

More accurate measurement of DLS can be achieved by using passive transmission methods such as the popular IEC-444 Pi-network (Fig. 17) widely used to measure the resonator motional parameters [13,20,32].

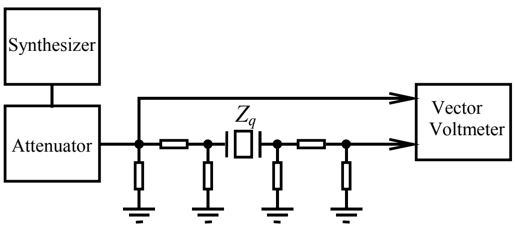

Figure 17: Simplified IEC-444 Pi-network crystal parameters measurement method [32].

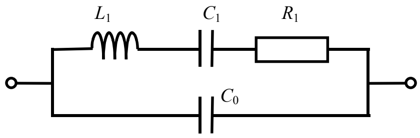

Figure 18: Crystal equivalent circuit.

The parameters of the resonator equivalent circuit (Fig. 18) can be calculated from the amplitude and phase transfer function of the measurement network the crystal is inserted in [28]. For high frequency resonators, those parameters can be obtained from the scattering parameters measurement by using automatic network analysers [1,23,24,25].
With the development of smart instrumentation and computer aided measurement techniques it is now very convenient to use network/impedance analysers that enable the user to vary several parameters such as the input signal magnitude and to calculate the equivalent circuit parameters from the impedance magnitude and phase records [18,19]. In the present case, the experiments have been performed by using an Agilent 4395A Network/Spectrum/Impedance Analyser and the 43961A Impedance Kit [22,33]. To improve the accuracy of the measurements, the resonator under test has to be isolated from the environmental perturbations mainly due to temperature fluctuations. To this end, the impedance test kit has been complemented with a precision oven keeping the crystal at its turnover point (Fig. 19, 20).

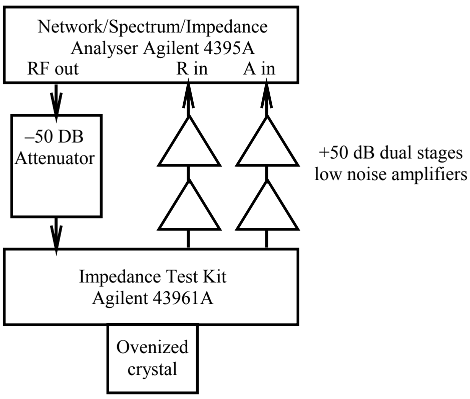

Figure 19: Low drive level crystal parameters measurement.

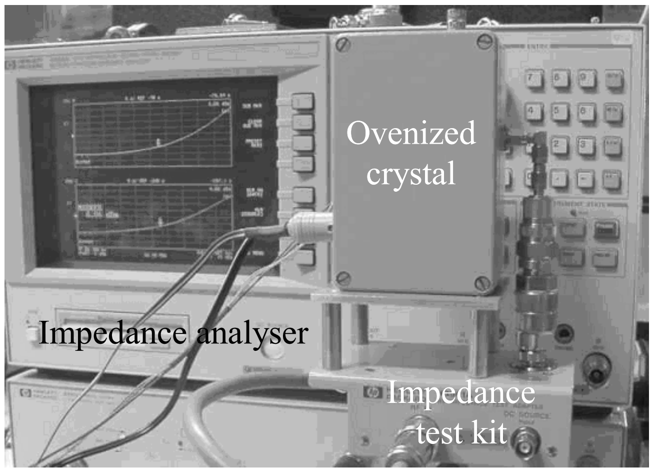

Figure 20: Experimental set-up.

Besides, so as to lower the drive level range initially set between – 50 to + 15 dBm, the experimental set-up has been modified as shown in Fig. 19: A wide band 50 dB attenuator is inserted in the RF input signal and two dual-stage low noise amplifiers are inserted in the measuring ports of the test kit allowing measurements from approximately – 100 dBm to - 35 dBm. It should be noted that a careful attention has to be paid to the calibration procedure to guarantee the measurement accuracy.
Figure 21 represents two typical records of the impedance the crystal parameters are calculated from. Of course, as the drive level decreases, the records become more and more noisy and several measurements are required to increase by averaging the signal to noise ratio. Figure 22 presents the drive level sensitivity of a 10 MHz SC-cut 3rd overtone quartz resonator. Nevertheless, the experimental set-up is not yet accurate enough to obtain satisfactory measurements of the crystal reactive parameters L_1 and C_1, and this plot is only a preliminary result that is still to be confirmed by additional experiments.

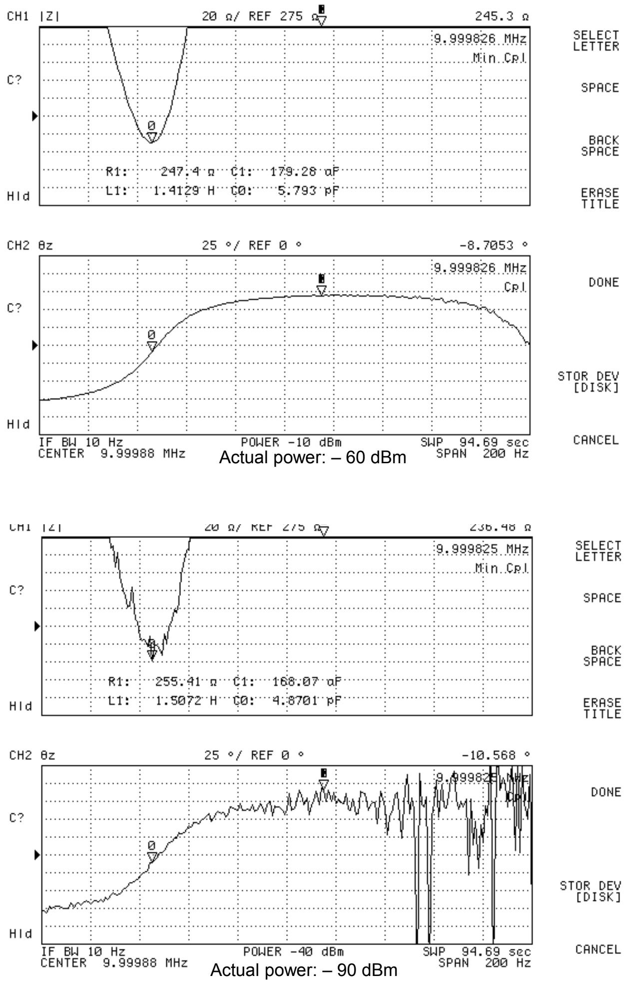

Figure 21: Low drive level crystal impedance records.

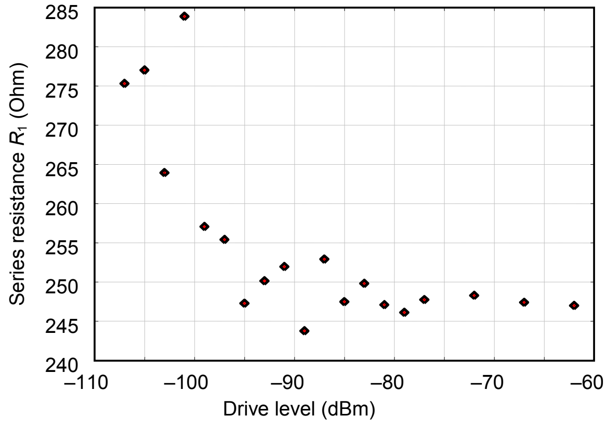

Figure 22: Low drive level sensitivity of a 10 MHz SC-cut 3rd overtone quartz resonator.

6 Noise and DLS

The main reason why these experiments are currently carried out is to check for a possible correlation between drive level sensitivity and noise of the resonators that should have the same origin. One of the possible mechanisms relating these two phenomena has been suggested in the past [30]. It assumed that some contaminant species are randomly trapped to and released from N possible surface sites at rates r_0 and r_1 respectively, each trapped particle causing an average relative frequency shift $\Delta f/f$ (Fig. 23).

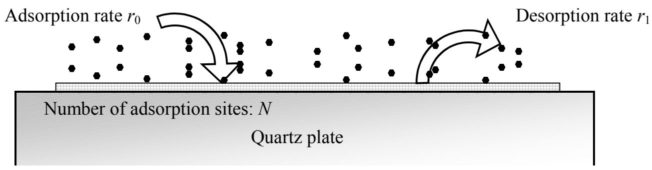

Figure 23: Noise induced by a contaminant species [30].

In this case it has been shown that the spectral density of phase fluctuations has the form given by Equation (12) represented in Fig. 24.

$$S_\phi(f) = \frac{8 r_0 r_1}{N(r_0 + r_1)} \left(\frac{\Delta f}{f}\right)^2 \frac{1}{(r_0 + r_1)^2 + (2\pi f)^2} \qquad (12)$$

Experimental verification of the expected correlation between drive level sensitivity and resonator noise has also been investigated [2,6]. The result presented in Fig. 25 seems demonstrate that there is a positive correlation between DLS measured by the slope of the resistance change and the noise measured by the residual phase noise at 100 Hz from the carrier [2].
Nevertheless, these promising results have not been confirmed by another set of experiments performed on a large sample of resonators as shown in Fig. 26 [6].

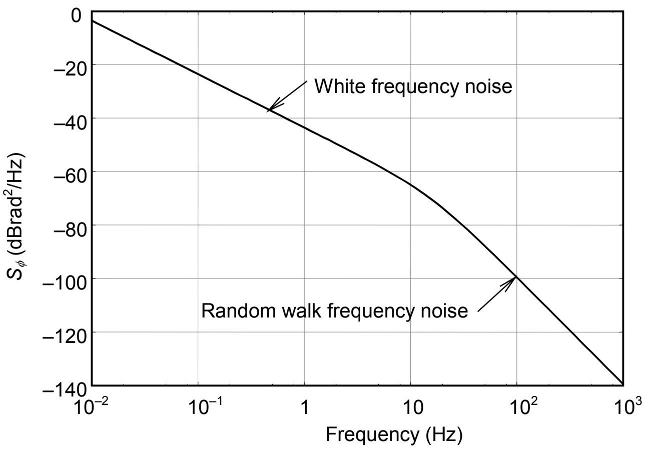

Figure 24: Spectral density of phase fluctuations for a 525 MHz resonator [30].

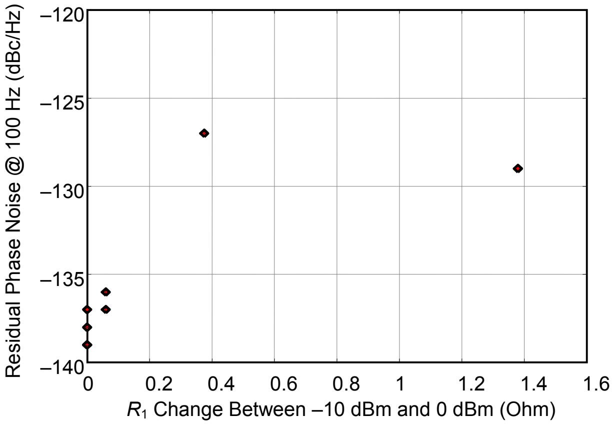

Figure 25: Noise vs. DLS of a 100 MHz AT-cut quartz [2].

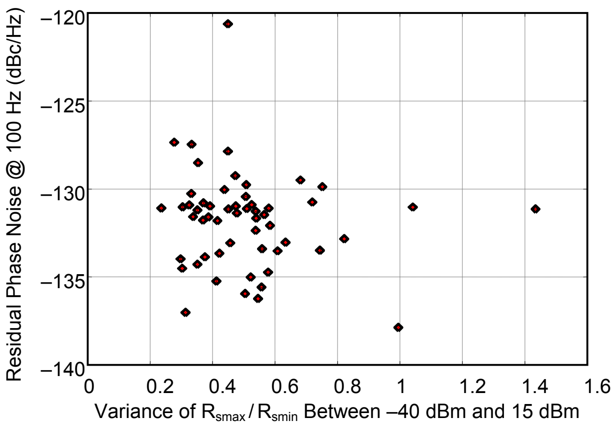

Figure 26: Noise vs. DLS of a 100 MHz AT-cut quartz [6].

Thus, the question of a possible correlation between noise and surface defects that could be disclosed by measuring DLS is still open. A theoretical noise model based on a non-linear series resistance R_1 (Fig. 18) whose value is a function or the crystal current as shown in Equation (13) has been introduced in the past [27] and is still under consideration [26].

$$R_1 = R_{10}\left(1+\frac{\gamma}{I^n}\right) \qquad (13)$$

In Equation (13):
R_{10} is the normal drive level resistance,
γ is the DLS coefficient,
I is the resonator drive current amplitude,
n is an integer number ($1 \le n \le 4$).

7 Conclusion

In summary, the low level drive sensitivity of quartz resonators is mainly expressed by a change of the series resonant frequency and series resistance that may exhibit various and often irreproducible behaviours. The correlation between DLS and surface defects is now well established and several models have been developed to describe the physical mechanism. Nevertheless, the question of the correlation between DLS and resonator noise is still open. Many other questions deserves careful attention such as:

– What happens at very low drive level, near the thermal noise floor?
– How behave the other motional parameters at these low drive level?
– Are the mechanisms responsible for the DLS the same as for the noise?
– How the assumed correlation can be demonstrated?

The work in progress will try to give an answer to these questions.

References

[1] J. P. Aubry, E. Gerard, S. Lechopier. “S. Y. Parameters Method for Accurate Measurements of Bulk Wave Crystal Resonators at Frequencies up to 2 GHz”, *Proc. 37th AFCS*, pp. 306–316, (1983).

[2] P. Bates. “Drive Level Dependence Versus Residual Phase Noise of Fifth Overtone AT Cut Quartz Crystals”, *Proc. 54th IEEE IFCS*, pp. 233–237, (2000).

[3] M. Bernstein. “Increased Crystal Unit Resistance at Oscillator Noise Level”, *Proc. 21st AFCS*, pp. 244–258, (1967).

[4] V. E. Bottom. “Introduction to Quartz Crystal Unit Design”, *Van Nostrand Reinhold Co.*, pp. 208–219, (1982).

[5] V. E. Bottom. “The Behavior of Quartz Resonators at Low Drive Levels”, *Proc. 5th Crystal Conference*, pp. 245–249, (1983).

[6] E. E. Carlson, T. E. Wickard. “A Study on the Measured Correlation of Drive Level Dependency and Phase Noise of Quartz Crystal Resonators”, *Proc. 55th IEEE IFCS*, pp. 338–344, (2001).

[7] R. C. Chittick, D. M. Hyland. “A Preliminary Investigation into a Novel Approach for the Removal of Drive Level Dependence in Quartz Crystal Resonators”, *Proc. 11th EFTF*, pp. 173–177, (1997).

[8] L. Dworsky, R. Kinsman. “A Simple Model for Quartz Resonator Low Drive Level Sensitivity and Monolithic Filter Intermodulation” *IEEE Trans. on UFFC*, **41** (2), pp. 261–268, (1994).

[9] G. L. Dybwad. “A sensitive New Method for the Determination of Adhesive Bonding Between a Particle and a Substrate”, *Journal of Applied Physics*, **58** (7), pp. 2789–2790, (1985).

[10] E. P. EerNisse. “An Analysis of Drive Level Sensitivity in Thickness Shear Quartz Resonators”, *Proc. 50th IEEE IFCS*, pp. 346–356, (1996).

[11] E. P. EerNisse, E. Benes, M. Schmid. “The Role of Localized Rotational Imbalance in Drive Level Dependence Phenomena”, *Proc. 56th IEEE IFCS*, pp. 2–7, (2002).

[12] E. A. Gerber. “VHF Crystal Grinding”, *Electronics*, pp. 161–163, (March, 1954).

[13] E. Hafner. “The Piezoelectric Crystal Unit – Definitions and Methods of Measurement”, *Proc. of the IEEE*, **57** (2), pp. 179–203, (1969).

[14] W. H. Horton, R. C. Smythe. “Experimental Investigations of Intermodulation in Monolithic Crystal Filters”, *Proc. 27th AFCS*, pp. 243–245, (1973).

[15] J. E. Knowles. “On the Origin of ‘Second Level of Drive’ Effect in Quartz Oscillators”, *Proc. 29th AFCS*, pp. 230–236, (1975).

[16] R. M. Lec, J. Sorial. “The Study of Colloidal Systems with TSM Piezoelectric Sensors”, *Proc. 55th IEEE IFCS*, pp. 838–845, (2001).

[17] L. Lindberg, G. Portnoff. “Test Oscillator for Study of Drive Level Dependence of Quartz Crystal”, *Proc. 48th IEEE IFCS*, pp. 273–280, (1994).

[18] H. Matthey. “Measurement of Crystal Parameters Using a Network Analyzer in Direct Impedance Mode”, *Proc. 7th EFTF*, pp. 177–180, (1993).

[19] P. E. Morley, R. J. T. Marshall, R. J. Williamson. “Crystal Parameter Measurement Using a Hewlett Packard HP4195A Network/Spectrum Analyzer”, *Proc. 3rd EFTF*, pp. 133–138, (1989).

[20] B. Neubig. “Measurement of Quartz Crystal Units up to 500 MHz and Above by the Use of a Pi Network with Error Correction”, *Proc. 11th Quartz Devices Conference*, pp. 60–68, (1989).

[21] S. Nonaka, T. Tuuki, K. Hara. “The Current Dependency of Crystal Unit Resistance”, *Proc. 25th AFCS*, pp. 139–147, (1971).

[22] K. Okada, T. Sekino. “The Impedance Measurement Handbook. A Guide to Measurement Technology and Techniques”, *App. Note No.* 5950-3000E, available from http://we.home.agilent.com, (2003).

[23] R. C. Peach, A. J. Dyer, A. Byrne, S. P. Doherty. “New Method for the Measurement of Quartz Crystal Resonator Parameters”, *Proc. 36th AFCS*, pp. 297–301, (1982).

[24] R. C. Peach, S. E. Morris. “A System for Precision Parameter Measurements on Quartz Crystal Resonators and Bipoles”, *Proc. 39th AFCS*, pp. 527–534, (1985).

[25] H. S. Pustarfi, W. L. Smith. “An Automatic Crystal Measurement System”, *Proc. 27th AFCS*, pp. 63–72, (1973).

[26] Y. S. Shmaliy, R. Brendel. “An Asymptotical Noise Model of a Crystal Oscillator with a Non-Linear Resonator”, in these proceedings.

[27] S. A. Trushliakov, Y. S. Shmaliy. “Influence of Equivalent Losses of Quartz Crystal Resonator on its Excitation in Oscillator”, *Radiotechnika*, **44** (7), pp. 41–44, (1989, in Russian).

[28] R. J. Williamson. “An Improved Method for Measuring Quartz Crystal Parameters”, *IEEE Trans. on UFFC*, **34** (6), pp. 681–689, (1987).

[29] J. S. Yerna. “Resistance – Measurement of Quartz Crystal at Very Low Drive Levels”, *Proc. 38th AFCS*, pp. 499–506, (1984).

[30] Y. K. Yong, J. R. Vig. “Resonator Surface Contamination – A Cause of Frequency Fluctuations?” *IEEE Trans. on UFFC*, **36** (4), pp. 452–458, (1989).

[31] Q. Zhang, R. Lec, K. Pourrezaei. “The Study of an Interaction of Solid Particles with Various Surfaces Using TSM Sensors”, *Proc. 57th IEEE IFCS*, pp. 1001–1006, (2003).

[32] “Basic Method for Measurement of Resonance Frequency and Equivalent Series Resistance of Quartz Crystal Units by Zero Phase Technique in a Pi_Network”, IEC Publication 444, (1973).

[33] “HP 4395A Network/Spectrum/Impedance Analyzer Operation Manual”, *Hewlett Packard Part No*. 04395-90000, (1997).